Chinese Journal of
POLYMER SCIENCE

ARTICLE

https://doi.org/10.1007/s10118-018-2120-0
Chinese J. Polym. Sci. 2018, 36, 925–933

Effect of a Hybrid Zinc Stearate-Silver System on the Properties of Polylactide and Its Abiotic and the Biotic Degradation and Antimicrobial Activity Thereof

Gabriela Jandíková, Petra Stoplova, Antonio Di Martino, Petr Stloukal, Pavel Kucharczyk*, Michal Machovsky, and Vladimir Sedlarik

Centre of Polymer Systems, University Institute, Tomas Bata University in Zlin, tr. Tomas Bati 5678, 760 01 Zlin, Czech Republic

Electronic Supplementary Information

Abstract This work investigates the degradation and properties of a thermoplastically prepared composite comprising a polylactide/hybrid zinc stearate-silver system. The influence of the zinc stearate-silver system on the properties of the composite is investigated by electron microscopy, differential scanning calorimetry and tensile tests. Furthermore, the antimicrobial activities of the systems are examined. The degradation behaviour of the composites is studied in both abiotic and biotic (composting) environments at an elevated temperature of 58 °C. The results reveal good dispersion of the additive in the PLA matrix, a stabilizing effect exerted by the same on the polylactide matrix during processing, and slight reduction in glass transition temperature. The zinc stearate-silver component also reduces brittleness and extends elongation of the composite. Abiotic hydrolysis is not significantly affected, which is in contrast with pure PLA, although mineralization during the early stage of biodegradation increases noticeably. The composite exhibits antimicrobial activity, even at the lowest dosage of the zinc stearate/silver component (1 wt%). Moreover, Ag and Zn contents were found to be present in the composite during abiotic hydrolysis, which was demonstrated by minimal diffusion of Ag ions from the matrix and very extensive washing of compounds that contained Zn.

Keywords Polylactide; Composite; Biodegradation; Zinc stearate; Silver; Antimicrobial

Citation: Jandíková, G.; Stoplova, P.; Di Martino, A.; Stloukal, P.; Kucharczyk, P.; Machovsky, M.; Sedlarik, V. Effect of a Hybrid Zinc Stearate-Silver System on the Properties of Polylactide and Its Abiotic and the Biotic Degradation and Antimicrobial Activity Thereof. Chinese J. Polym. Sci. 2018, 36(8), 925–933.

INTRODUCTION

Polylactide (PLA) has been widely investigated as it constitutes a polymer with potential for application in food packaging, medicinal and especially hygienic materials. However, such applications require good mechanical properties and other specific qualities, such as antimicrobial activity. Therefore, modifications to engender lower brittleness and higher elongation are necessary.

The improvement of mechanical properties accompanied by preservation of full biodegradability can be achieved through several ways. The most effective ways are: (i) chain orientation[1], (ii) blending it with other biodegradable polymers[2], or (iii) by introducing plasticizer systems into it[3]. Examples of suitable polymers with the capacity to blend with PLA in order to improve flexibility are thermoplastic starch[4], poly(ethylene oxide)[5, 6], poly-(ethylene glycol)[6], poly(ε-caprolactone)[7] and cellulose acetate[8]. Common plasticizers able to effectively increase elongation include glycerol, triacetin, low-molecular-weight citrates and partial fatty acid esters[3].

Antimicrobial modifications to polymers are made to prevent or inhibit the growth of microorganisms on the surface. Presently, a popular method for modifying polymers is the addition of an antimicrobial agent/additive directly into the polymer matrix. To date, silver and zinc based additives have received particular attention, due to the low toxicity of the active Ag ion to human cells, as well as for being a long-lasting biocide with high thermal stability and low volatility[9, 10]. So as to achieve good dispersion of silver particles in the polymer matrix and consequently increase antimicrobial activity, Ag particles are often immobilized into a suitable substrate. This also facilitates the handling and mixing process[11, 12].

For example, the immobilization of Ag-NPs by microwave synthesis onto various organic substrates was studied by Bazant *et al*[11]. The authors successfully immobilized nanosilver, nanostructured ZnO and hybrid nanostructured Ag/ZnO onto a wood flour surface by

* Corresponding author: E-mail p.kucharczyk@seznam.cz

Received December 2, 2017; Accepted February 3, 2018; Published online April 20, 2018

microwave synthesis. Subsequently, the modified wood flour was compounded into a PVC matrix (5 wt% loading) and antimicrobial activity was tested; the most efficient system was a hybrid nanostructured Ag/ZnO system. Iqbal *et al*. described surface modification by microwave synthesis of Ag-Nps on the surfaces of inorganic substances[10]. Such Ag-NPs were successfully bonded onto hydroxyapatite, initiating antimicrobial activity in the given system. Pantani *et al*.[14] prepared PLA/ZnO based nanocomposites that exhibited good antimicrobial activity. However, they reported that the parameters of certain mechanical properties, such as elongation at yield and break, required improvement by adding a plasticizer into the nanocomposite film.

With this in mind, the objective of the work herein was to prepare PLA-based composites with an additive that fulfilled both functions: fragility suppression and demonstration of antimicrobial activity. To this end, Ag nanoparticles were immobilized by microwave synthesis on the surface of zinc stearate (ZnSt), and the resulting hybrid system (ZnSt-Ag) was incorporated into the PLA polymer matrix at various concentrations. Investigation was made into changes in thermal and mechanical properties, as well as the morphology of the composites pertaining to their dependence on the given concentration of ZnSt-Ag. Moreover, the influence of the ZnSt-Ag system on the degradation behaviour of the PLA was observed during abiotic and biotic (composting) hydrolysis, which represents an important means of depolymerizing PLA.

EXPERIMENTAL

Materials

The polylactide was obtained from NatureWorks (Ingeo™ 4060D). Its weight-average molar weight (M_w) was 1.58 × 10^5 g·mol^{-1} and molar mass dispersity index equalled 3.5, as determined by GPC according to the method described below. Zinc stearate (ZnSt) was supplied by Sigma Aldrich (USA). Silver nitrate ($AgNO_3$), hexamethylenetetramine (HMTA), dimethylformamide (DMF) and ethanol were purchased from Penta (Czech Republic).

Sample Preparation

Preparation of hybrid ZnSt-Ag particles

These were prepared under reflux in the MWG1K-10 microwave open vessel system (RADAN, Czech Republic; 1.5 kW, 2.45 GHz), operating in continuous mode (zero idle time) with an external cooler. Firstly, 200 mL of $AgNO_3$ (0.85 g) solution in water and 450 mL of ZnSt (11.02 g) dispersion in ethanol were transferred into a 1000 mL reaction bottle.

The reaction mixture was heated in a microwave oven for 2 min. Afterwards, 100 mL of HMTA (7.00 g) solution in water was added; then heating continued for 10 min under continuous stirring (250 r·min^{-1}). The reaction product was collected, filtered and left to dry in a laboratory oven (50 °C) until constant weight was achieved. The ZnSt-Ag system thus prepared contained 4.09 wt% Ag, as determined on an energy dispersive X-ray fluorescence spectrometer under the conditions described below.

Preparation of PLA/ZnSt-Ag mixture

Prior to being compounded, the PLA pellets were dried at 45 °C under reduced pressure (1 kPa) for 24 h. Said hybrid particles were incorporated into the PLA matrix by a co-rotating twin screw micro-compounder, of type MiniLab II HAAKE Rheomex CTW5 (Thermo Scientific, Germany, 5 mL chamber volume). The temperature during the mixing process was set to 180 °C; the screw speed was 100 r·min^{-1} and the duration of such mixing lasted 5 min. The concentrations of the ZnSt-Ag equalled 1 wt%, 3 wt%, 5 wt% and 10 wt% according to the weight of the PLA.

The authors prepared PLA films that were 500 μm thick by compression moulding. This involved heating the material to 180 °C for 1 min, then moulding it for 2 min, followed by immediately cooling the same in a second cold press maintained at 20 °C.

Characterization Methods

Gel permeation chromatography (GPC)

GPC analysis was conducted on an HT-GPC 220 chromatographic system (Agilent), equipped with a dual detection system (refractive index and viscometric response detectors). The samples were dissolved in THF (~3 mg·mL^{-1}) overnight. Separation and detection took place on PL gel-mixed bed columns (1x Mixed-A, 300 × 7.8 mm, 15 μm particles + 1x Mixed-B, 300 × 7.8 mm, 10 μm particles + 1x Mixed-D, 300 × 7.8 mm, 5 μm particles) at 40 °C in THF; the flow rate equalled 1.0 mL·min^{-1} and injection volume was 100 μL. The GPC system was calibrated through universal calibration with narrow polystyrene standards ranging from 580 g·mol^{-1} to 6.00 × 10^6 g·mol^{-1} (Polymer Laboratories Ltd., UK). The weight-average molecular weight M_w, number-average molecular weight M_n and molar-mass dispersity ($Đ = M_w/M_n$) of the tested samples were determined from peaks corresponding to the polymer fraction. All data processing was carried out using Cirrus software.

Mechanical properties

The tensile tests of the composites were carried out according to the CSN EN ISO 527-1-4 standard on a tensile testing machine, the Testometric M350-5CT (United Kingdom), at a crosshead speed of 5 mm·min^{-1}. The dimensions of dog-bone form specimens cut from the compression moulded plates measured 60 mm × 4.0 mm × 0.5 mm. Prior to testing, all the samples were readied under conditions of 22 °C and 64% relative humidity for 24 h. At least seven specimens from each group were tested.

Scanning electron microscopy (SEM)

The structure of the prepared samples was observed by scanning electron microscopy (VEGA IILMU, TESCAN). The sample of neat additive was analysed as prepared, without an Au-Pd layer. The microscope was operated in vacuum mode at an acceleration voltage of 10 kV.

Energy dispersive X-ray fluorescence spectroscopy (EDXRF) analysis of composites during hydrolysis

In order to determine the Ag and Zn contents in the prepared ZnSt-Ag system, the authors carried out EDXRF analysis. Such measurement was performed on a spectrometer (ARL Quant'X EDXRF Analyzer, Thermo Scientific, Germany).

https://doi.org/10.1007/s10118-018-2120-0

Pieces of the solid samples (approx. 30 mg) were dissolved in 4 mL of DMF and analysed by EDXRF under the following conditions: all measurements were carried out in an air atmosphere and any X-rays emitted were detected by an electrically cooled Si(Li) detector. The energy resolution was 50 kV for Ag and 20 kV for Zn in the duration of 60 s. The concentrations of Ag and Zn were derived from calibration curves obtained under the same conditions, ranging between 0−250 mg·L^{-1}; certified reference standards were applied for such calibration.

Antimicrobial activity

Antimicrobial testing was performed on the films according to the ISO 22196:2007 international standard. Such activity was tested against the bacteria strains *Escherichia coli* (Gram-negative) and *Staphylococcus aureus* (Gram-positive). Colony forming units (CFU) were determined, and antimicrobial activity (R) was defined as differences between logarithmic values for growth in treated and untreated samples according to Eq. (1)

$$R = U_t - A_t \quad (1)$$

where U_t is the average of the common logarithm for the number of viable bacteria, in cells per cm^2, recovered from untreated test specimens after 24 h; A_t stands for the average of the common logarithm for the number of viable bacteria, in cells per cm^2, recovered from treated test specimens after 24 h; and R is antibacterial activity.

Reduction in the colony forming units (CR) is expressed by reduction in the number of the colonies formed per cm^2 in per cent, according to Eq. (2)

$$CR = \left(1 - \frac{N_S}{N_B}\right) \times 100 \quad (2)$$

where N_B is the number of viable colonies per cm^2 recovered from the material without the additive (blank) after 24 h, and N_S is the number of viable colonies per cm^2 recovered from samples containing antimicrobial agents after 24 h.

Abiotic degradation

The samples (approx. 50 mg) were cut into 0.3 cm × 0.5 cm specimens, which were subsequently placed in a 25 mL glass bottle, fully immersed in a hydrolysis medium (sodium phosphate buffer 0.1 mol·L^{-1}, pH = 7, with the antimicrobial growth inhibitor NaN_3, 0.2 wt%) and shaken. At each follow-up time, a specimen was removed and analysed by GPC. Hydrolysis was performed at the temperature of 58 °C.

Biodegradation in compost

The method applied was consistent with those described in certain references[15, 16]. 50 mg of dry material, 5 g of perlite and 2.5 g of dry-weight compost were weighed into each 500 mL biometric flask. The flasks were sealed with stoppers equipped with septa and incubated at 58 °C. Head-space gas was sampled at appropriate intervals through the septum with a gas-tight syringe, and then injected manually into a GC instrument (GC-2010 Plus, Shimadzu), equipped with Porapak Q (1.829 m length, 80/100 MESH) and 5Å-molecular-sieve (1.829 m length, 60/80 MESH) packed columns connected in series, as well as a thermal conductivity detector (carrier gas helium, flow 53 mL·min^{-1}, column temperature 60 °C). The concentrations of CO_2 and O_2 were derived from the calibration curve obtained using a calibration gas mixture of declared composition (Linde). Endogenous production of CO_2 by soil or compost in blank incubations was always subtracted to obtain values representing net sample mineralization. The blank sample comprised 2.5 g of compost matter without any polymer sample; hence its production of CO_2 pertained entirely to the compost. From the concentration found, the percentage of mineralization with respect to the initial carbon content of the sample was calculated according to Eq. (3):

$$M(\%) = \frac{m_{gc}}{m_s \cdot w_c} \quad (3)$$

where M is the percentage of mineralization, m_{gc} is the mass of carbon evolved as CO_2 and obtained from GC analysis, m_s is the weight of the polymer sample, and w_c is the percentage (W/W) of carbon in the polymer investigated. Values of w_c for the given materials were determined on a total organic carbon (TOC) analyser (TOC-L, Shimadzu), equipped with a solid sample module (SSM-5000A, Shimadzu). In parallel, oxygen concentration was also monitored to provide a control mechanism so as to ensure that samples did not suffer from hypoxia. Three parallel flasks were run for each sample, along with four blanks.

Differential scanning calorimetry (DSC)

Thermal properties were investigated by DSC using a DSC1 STAR System (Mettler Toledo, Switzerland). Samples with a weight of *ca*. 8−11 mg were placed in aluminium pans. A nitrogen flow of 50 mL·min^{-1} was set, and the following heating program was applied: an initial heating cycle from 0 °C to 200 °C (10 °C·min^{-1}), maintaining the same for 2 min and cooling to 0 °C (10 °C·min^{-1}). Afterwards, the temperature of 0 °C was held for 2 min and a second heating scan performed to 200 °C. Melting point temperature (T_m) and the related value of enthalpy were obtained from the first heating cycle. The region of glass-transition temperature (T_g) was determined from the second heating scan. Crystallization temperature (T_c) was detected from cooling scan.

RESULTS AND DISCUSSION

Additive and Composite Morphology

The morphology of the prepared ZnSt-Ag additive was investigated by SEM. As can be seen in Figs. 1(a) and 1(b), no significant differences between the structures of the additives were discerned, in addition to which crystals of zinc stearate at the scale of micrometres were observed. However, detailed SEM-EDX analysis (displayed in Figs. S1 and S2 in the electronic supplementary information, ESI) showed that Ag was undoubtedly present on the surface of the ZnSt-Ag additive.

Analysis was made on white spots of size less than 100 nm adhered to the surface of the ZnSt-AG (Fig. 1a), and they were found to be a chlorine impurity (Fig. S1, in ESI), most probably AgCl.

The size and shape of the prepared Ag-NPs correspond to the results published by Bazant *et al.*[11], in which Ag-NPs were immobilized on a wood flour surface. The SEM micrographs of the PLA 0%, 3% and 10% ZnSt-Ag

https://doi.org/10.1007/s10118-018-2120-0

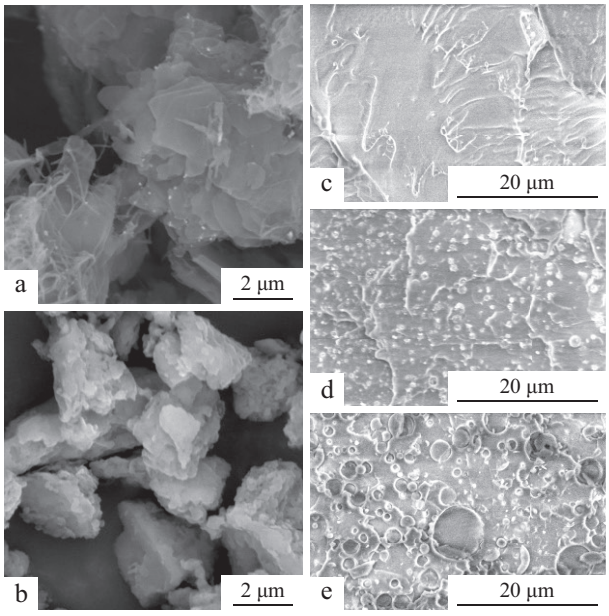

Fig. 1 Scanning electron micrographs of (a) the prepared ZnSt-Ag system, (b) reference zinc stearate without Ag, (c) PLA 0 wt% ZnSt-Ag composite, (d) PLA 3 wt% ZnSt-Ag composite, (e) PLA 10 wt% ZnSt-Ag composite

composites taken from the cold fracture of tensile specimens are shown in Figs. 1(c)−1(e). It was revealed that the additive was relatively well dispersed in the PLA matrix, forming droplets variable in size (less than 5 μm).

Elemental Composition

Table 1 summarizes the basic compositional and physico-chemical properties of the prepared composites with the ZnSt-Ag additive. As expected, the greatest Ag/Zn concentration, 0.44/1.06 wt%, was detected in the sample with the highest loading, *i.e.* 10 wt% ZnSt-Ag. The composites with 1 wt%, 3 wt% and 5 wt% of ZnSt-Ag contained 0.04/0.11, 0.14/0.32 and 0.26/0.56 wt% of Ag and Zn, respectively.

Processing Stability

PLA is sensitive to increased temperatures and during processing is subjected to thermal degradation. This is further enhanced by such phenomena as the presence of moisture, a residual catalyst, plasticizers, a monomer and fillers. It is known that at processing temperatures (190−240 °C) primary degradation mechanisms take the form of backbiting (intramolecular termination) and inter-esterification reactions (schematically depicted in Figs. 2a and 2b), which can be catalysed by such means as a residual catalyst or by incorporating metals into the matrix. The first of the two (Fig. 2a) leads to extensive formation of lactide, whereas the latter (Fig. 2b) brings about molecular weight loss and redistribution[17–20].

The GPC results presented in Table 1 reveal significant reduction in molecular weight in all the samples after processing. Interestingly, increasing the concentration of the ZnSt-Ag component exerted a favourable effect on PLA molecular weight reduction, with the lowest extent of degradation being observed under circumstances of the highest additive content (10%).

The effect of metal stearates on PLA has not been previously investigated in the literature, so it is possible that the stabilizing effect observed was caused by either i) mutual reactions between the carboxylic chain ends of the PLA and zinc stearate (see Figs. 2c and 2d), which are based on the recognized acid scavenger activity of ZnSt[21–23]; or ii) by mutual reactions between the hydroxylic chain ends of the PLA and zinc stearate (see Figs. 2e and 2f). The latter was assumed to be analogous to the description by Costa *et al*[24]. Both reactions would trigger general redistribution of molecular weights and reduce intermolecular-esterification reactions (Fig. 2b) due to neutralization of OH end groups by the zinc stearate. One might expect that the presence of zinc compounds would increase degradation due to the effective catalysis of back-biting and transesterification reactions. However, it seems that the stabilizing effect is dominant in these systems. This theory is backed up by a study by Cam *et al*.[25], who found that zinc ions exert a relatively limited decomposing effect on the PLA matrix.

Thermal Properties

The thermal behaviour of the investigated samples and pure ZnSt-Ag additive were analysed by DSC and data are summarized in Table 1. Raw thermograms can be found in supplementary data file as Figs. S3−S6 (in ESI). It was found that the neat PLA possessed an amorphous character with a glass transition temperature (T_g) of around 56 °C. The composites with ZnSt-Ag exhibited a slightly diminished T_g of around 51 °C. This reduction can be attributed to the presence of zinc stearate chains, which probably increased the free volume of the PLA amorphous phase, hence lower T_g values were observed. Simultaneously, PLA degradation during processing further contributed to the lower T_g values, since chain cleavage produces more chain end groups that in

Table 1 Material properties of PLA/ZnSt-Ag composites

Sample	Ag measured [b] (wt%)	Zn measured [b] (wt%)	M_w [c] (kg·mol^{-1})	$Đ$ [d]	T_g [e] (°C)	T_c [f] (°C)	ΔH_c [g] (J·g^{-1})	T_m [h] (°C)	ΔH_m [i] (J·g^{-1})
PLA [a]	n.d.	n.d.	122	2.78	55.8	–	–	n.d.	n.d.
PLA + 1 wt% ZnSt-Ag	0.04	0.11	74	2.49	50.8	–	–	n.d.	n.d.
PLA + 3 wt% ZnSt-Ag	0.14	0.32	81	2.64	51.2	65.4	0.87	116.4	0.75
PLA + 5 wt% ZnSt-Ag	0.26	0.56	94	2.08	51.8	66.4	2.67	116.8	2.10
PLA + 10 wt% ZnSt-Ag	0.44	1.06	99	2.51	51.6	72.1	6.13	117.5	5.37
ZnSt-Ag	4.09	9.89	n.d.	n.d.	n.d.	86.1	128.17	118.4	169.07

[a] Neat processed PLA without ZnSt-Ag; [b] Concentration of Ag and Zn as analysed by EDXRF; [c] Weight-average molecular weight; [d] Molar-mass dispersity; [e] Glass transition temperature of the PLA phase; [f] Crystallization temperature; [g] Enthalpy of crystallization; [h] ZnSt-Ag melting temperature; [i] Enthalpy of melting; n.d., not detected.

https://doi.org/10.1007/s10118-018-2120-0

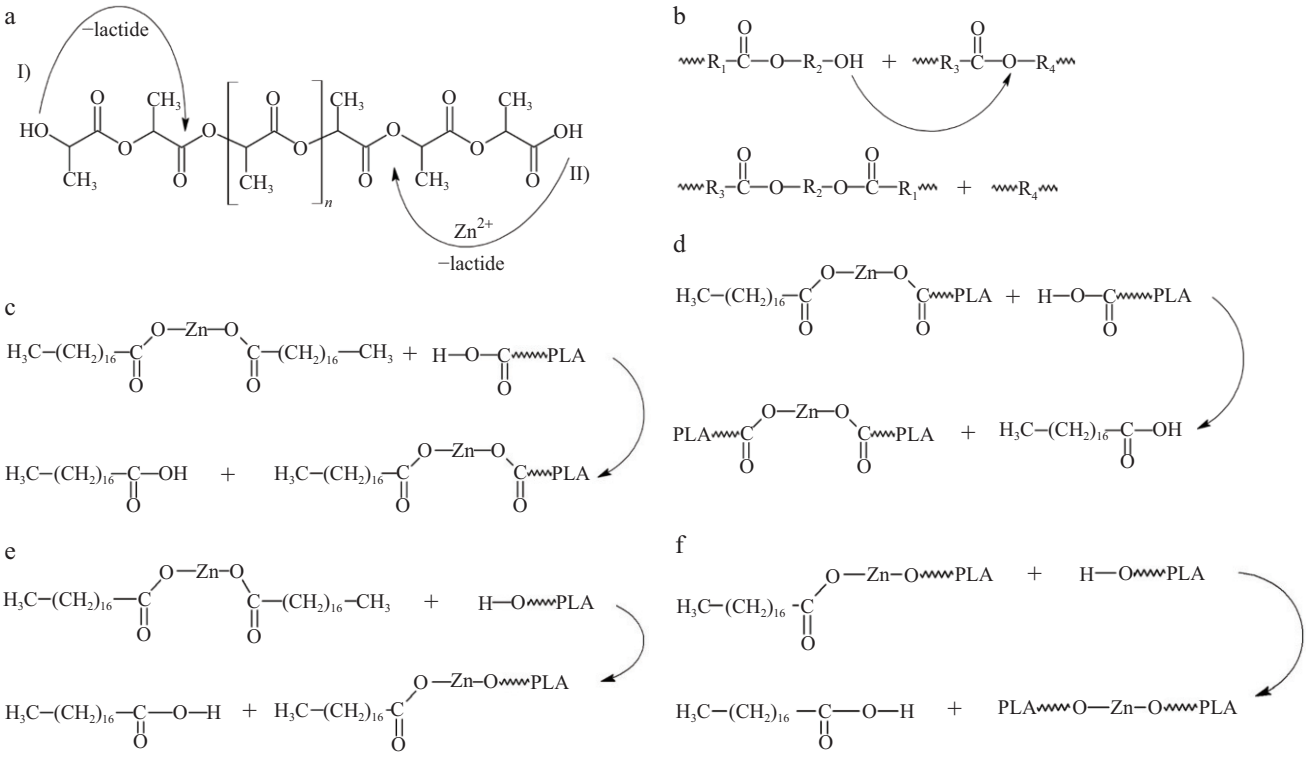

Fig. 2 Possible reactions during blend mixing, stoichiometry omitted (R represents various PLA segments): (a) Backbiting reaction leading to lactide formation; (b) Inter-esterification reaction leading to molecular weight degradation; (c, d) The two-step reaction of zinc stearate with PLA chains *via* free carboxylic end groups; (e, f) The two-step reaction of zinc stearate with PLA chains *via* free hydroxylic end groups

turn increases free volume and a shift in the mobility of the chain towards lower temperatures[26].

A melting temperature (T_m) was not observed for the neat PLA sample, meaning that the polymer did not crystallize when cooling after it had been processed, a phenomenon which is often seen in PLA[23, 24]. The lowest concentration of ZnSt-Ag brought about the same results, although raising the amount of ZnSt-Ag led to observation of a melting endotherm with a peak value of approximately 116 °C in the first DSC scan, most likely a consequence of the ZnSt-Ag melting which was detected at 118.4 °C (Fig. S6, in ESI). An interesting finding was that during cooling scan an exothermal signal around 65 °C was detected. Most probably this signal was attributed to crystallization temperature (T_c) of ZnSt-Ag additive. Observed temperatures were lower than those detected in pure ZnSt-Ag (86.1 °C) and are presented in Table 1 and Fig. S6 (in ESI). The reduced T_c of ZnSt-Ag was caused by the presence of PLA chains which blocked crystallization of ZnSt-Ag at higher temperatures.

Mechanical Properties

Tensile properties are displayed in Figs. 3(a)−3(c). As shown in Fig. 3(a), adding just 1% ZnSt-Ag into PLA produced nearly a 50% decrease in Young's modulus. This value remained fairly steady despite further experimentation with increasing the concentration of ZnSt-Ag. Tensile strength

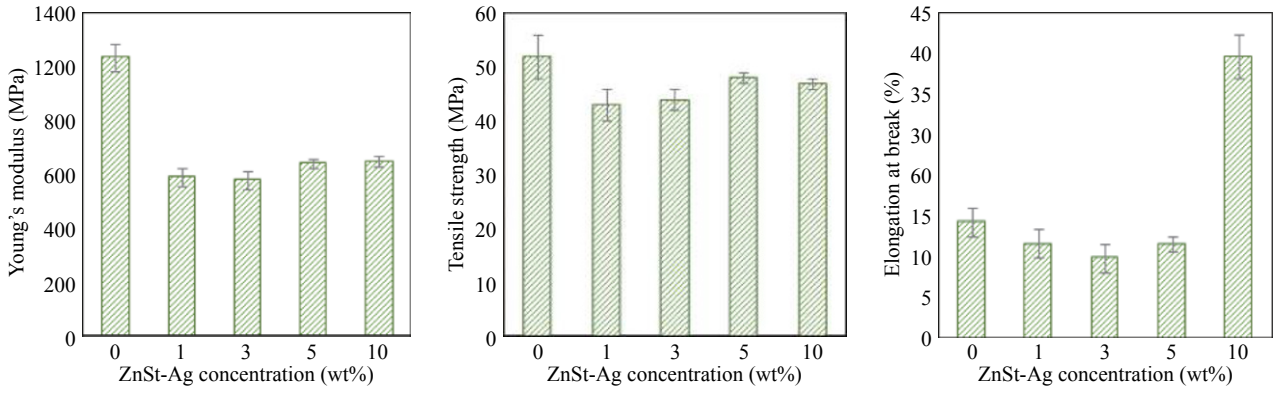

Fig. 3 Mechanical properties of PLA and PLA/ZnSt-Ag composites: (a) Young's modulus; (b) Tensile strength; (c) Elongation at break

https://doi.org/10.1007/s10118-018-2120-0

decreased from the initial figure of 52 MPa to a level between 43–48 MPa; greater values were observed in samples with a higher concentration of the additive (Fig. 3b). The reduction in Young's modulus and tensile strength was attributed to the presence of the dispersed additive in the PLA matrix, which affects its homogeneity and consequently diminishes the tensile strength of the prepared composites. The lower tensile strength witnessed for all the PLA/ZnSt-Ag blends might also have resulted from decrease in the molecular weight (M_w) of the polymer chain. The shorter the polymer chain is, the fewer the entanglements of the polymer chain, leading to low strength-at-break. Interesting phenomena were observed for elongation at break (Fig. 3c). While a slight drop-off was detected from the initial 15% recorded for neat PLA to around 12% in the case of 5% PLA/ZnSt-Ag, the sample containing 10% ZnSt-Ag exhibited completely different behaviour. In this instance, significant enhancement in elongation (nearly 40%) was measured. This indicated that ZnSt-Ag reduced intermolecular forces and overall cohesion between polymer chains and increased the mobility of PLA chains, thus enhancing flexibility. Potentially, this was caused by the presence of the long-chain hydrocarbon portions of stearate, and similar behaviour has also been observed by other authors[27, 28].

Antimicrobial Properties

The antimicrobial activities of the PLA-based composite films against *E. coli* (Gram-negative) and *S. aureus* (Gram-positive) bacterial strains are given in Table 2. The number of colony forming units per cm^2 of sample (N) was determined, while the antibacterial activity (R) and percentage of reduction in colony forming units (CR) were estimated. As expected, distinct antimicrobial activities were exhibited by the films with the highest Ag loading. Activity was stronger against *E. coli* than *S. aureus*, which is in agreement with results published by Shankar *et al*[29]. Said authors described the significant antimicrobial activity of PBAT-based composites with a similar concentration (0.25 wt%) of Ag, in which such activity was also higher against Gram-negative bacteria[29]. According to the CR results, it remains significant that lesser growth of microbial cells was observed in the remaining samples with 1 wt%, 3 wt% and 5 wt% ZnSt-Ag, where reduction (in per cent) in the colony forming units per cm^2 was seen to range between approximately 25% to 70%.

It is a well-known fact that Gram-negative bacteria strains are more sensitive to the action of Ag NPs than Gram-positive strains. Several mechanisms of Ag NPs have previously been reported, although a clear mechanism has yet to be established. The most widely accepted mechanism that has been proposed describes the interaction of Ag with the negatively charged phosphorous in bio-macromolecular compounds containing sulphur (proteins and nucleic acids), which causes structural changes and deformation of metabolic processes, leading to cell death[30].

Abiotic Degradation

The sensitivity of PLA to abiotic hydrolysis is considered as a limiting factor for long-term service applications. Consequently, the effect of ZnSt-Ag on the rate of hydrolysis was investigated by GPC.

The changes in weight-average molecular weight (M_w) during hydrolysis at 58 °C are shown in Fig. 4, while the kinetic constants are summarized in Table 3. As can be seen, all the samples incorporating neat PLA exhibited a drop in M_w within the first few days of the experiment. According to degradation constant (u) presented in Table 3, no significant differences in hydrolysis rate were observed, although the actual values for M_w varied due to difference in the initial ones (M_{w_0}). The fact that no significant changes were exhibited indicated that the ZnSt-based additive did not possess any hydrolysis retardation or did not exert any activation effects at the elevated temperature of 58 °C, in contrast with neat PLA.

These findings were notable since either of the following might potentially happen: i) retardation could be expected

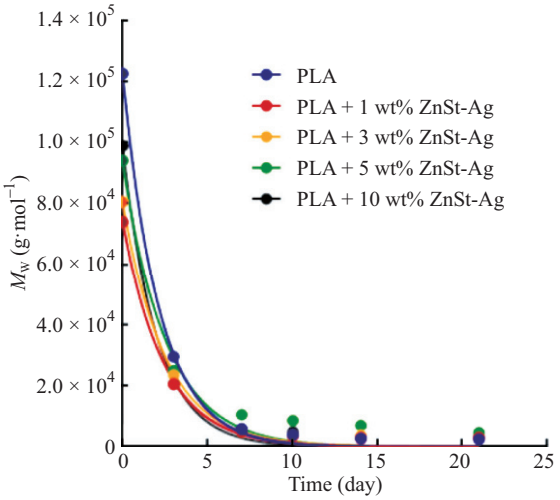

Fig. 4 Molecular weight evolution of neat PLA and PLA-based composites during abiotic hydrolysis in 0.1 mol·L^{-1} phosphate buffer (pH = 7) at 58 °C

Table 2 Antimicrobial activity of the prepared composites determined according to ISO 22196

Sample	*Staphylococcus aureus* CCM 4516			*Escherichia coli* CCM 4517		
	N (cfu·cm^{-2})	CR (%)	R	N (cfu·cm^{-2})	CR (%)	R
PLA [a]	2.4×10^5		$U_t = 5.4$	1.2×10^6		$U_t = 6.1$
PLA + 1 wt% ZnSt-Ag	1.5×10^5	38	0.21	9.2×10^5	23	0.13
PLA + 3 wt% ZnSt-Ag	1.6×10^5	33	0.17	3.6×10^5	70	0.53
PLA + 5 wt% ZnSt-Ag	6.5×10^4	73	0.56	6.0×10^5	50	0.32
PLA + 10 wt% ZnSt-Ag	1.1×10^1	100	4.32	< 1	100	> 6.1

[a] Neat processed PLA without ZnSt-Ag

https://doi.org/10.1007/s10118-018-2120-0

Table 3 First-order kinetic model parameters and coefficients of determination (R^2) for random scission of the PLA and PLA nanocomposites

Sample	M_{w_0} [a] (kg·mol^{-1})	u [b] (day^{-1})	R^2
PLA	122 ± 2	0.464 ± 0.026	0.998
PLA + 1 wt% ZnSt-Ag	74 ± 2	0.410 ± 0.035	0.994
PLA + 3 wt% ZnSt-Ag	80 ± 3	0.399 ± 0.032	0.995
PLA + 5 wt% ZnSt-Ag	93 ± 6	0.389 ± 0.064	0.975
PLA + 10 wt% ZnSt-Ag	99 ± 4	0.499 ± 0.053	0.993

[a] Initial weight average M_w at time $t = 0$; [b] Rate constant of abiotic hydrolysis; details on the model used can be found in a previous work by the authors[14].

due to the hydrophobic nature of ZnSt, which would likely cause decrease in water absorption; ii) the acceleration might have been caused by the catalytic effect of zinc on ester bond hydrolysis. However, none of these phenomena were observed under the experimental conditions.

Biodegradation

The samples of the studied materials, comprising different compositions, underwent biodegradation tests simulating decomposition of the materials under composting conditions at 58 °C (Fig. 5). All the investigated samples achieved nearly 100% mineralization after 90 days of incubation, indicating that they were easily biodegraded in a composting environment. It was observed that the presence of the ZnSt-Ag additive slightly promoted biodegradation, while faster rate constants (k_{aqc}) and onsets (C) were also detected (data shown in Table 4). It should be noted that biodegradation in this experiment was evaluated on the basis of the CO_2 evolved by the microorganisms; therefore, the extent of the same depends on the concentration of low molecular weight fragments able to diffuse out from the matrix. The more rapid biodegradation of samples containing ZnSt-Ag was attributed to the following phenomena: i) the composites possessed lower T_g, hence faster diffusion of low molecular weight products was possible through the matrix; ii) due to the high temperature of the experiment, the hydrophobic ZnSt phase started to migrate and concentrate on the surface of the sample, where it could easily be assimilated by microorganisms.

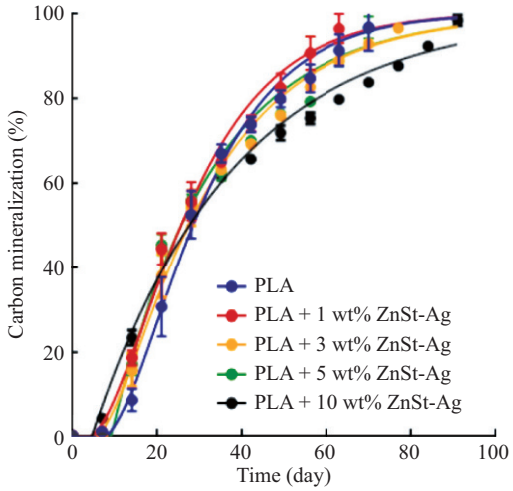

Fig. 5 Comparison of the biotic degradation of PLA and modifications made to the same by ZnSt-Ag over time at 58 °C

The second interesting behaviour observed pertained to the sample with 10% additive, in which biodegradation suddenly slowed down at around the midway point of the experiment. This could not be fully explained by the authors, because at this phase of biodegradation the molecular weight of all the samples should have been very low (on the basis of the abiotic experiment depicted in Fig. 4). It might have been caused by increased toxicity resulting from the large amount of ZnSt additive utilized and its degradation product, *i.e.* ZnO resulted from hydrolysis of ZnSt. ZnO was found to be toxic to some environmental microorganisms isolated from soil and sewage[31, 32].

Release of Silver and Zinc

The changes in Ag and Zn concentrations in the composites during abiotic hydrolysis were measured by EDXRF and are shown in Figs. 6 and 7, respectively. It was noticeable that the concentration of Ag exceeded the initial value through continuous degradation. This shows that the diffusion of degraded PLA chains was much more rapid than the diffusion of Ag from the polymer composite into the surrounding environment. In other words, the mobility of Ag in the composite was smaller than the mobility of the PLA chains, even after they had cleaved into short oligomers. Therefore, a rise in concentration of Ag was detected. In the case of Zn, different behaviour was observed. Initially, although a small increase was witnessed, after ten days, the

Table 4 Kinetic model parameters and coefficients of determination (R^2) for the biodegradation of pure PLA and PLA + ZnSt-Ag additive films

Sample	$C_{aq,0}$ [a] (%)	$C_{h,0}$ [b] (%)	k_{aqc} [c] (day^{-1})	k_h [d] (day^{-1})	C [e] (day)	R^2
PLA	0	100	0.078	0.078	6.8	0.979
PLA + 1 wt% ZnSt-Ag	0	100	0.076	0.076	3.44	0.972
PLA + 3 wt% ZnSt-Ag	0	100	0.172	0.043	4.91	0.984
PLA + 5 wt% ZnSt-Ag	0	100	0.770	0.042	3.77	0.958
PLA + 10 wt% ZnSt-Ag	0	100	3.082	0.030	4.22	0.985

[a] Percentage of initial intermediate solid carbon; [b] Percentage of initial hydrolyzable solid carbon; [c] Rate constant for mineralizing water-soluble carbon into carbon dioxide; [d] First-order hydrolysis rate constants; [e] Duration of lag phase during the initial phase of biodegradation before the onset of CO_2 production; Details on the model used can be found in a previous work by the authors[14].

https://doi.org/10.1007/s10118-018-2120-0

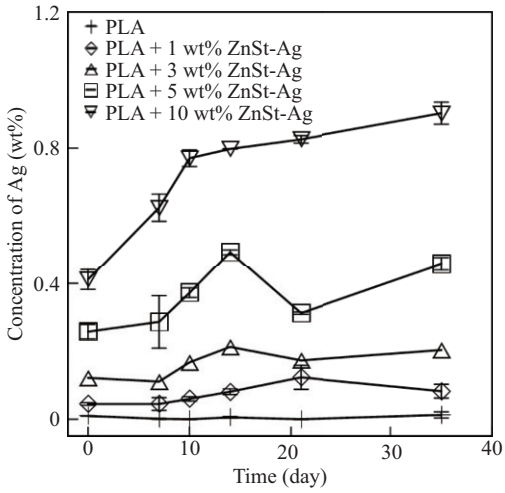

Fig. 6 Concentration of Ag in the composites during abiotic hydrolysis

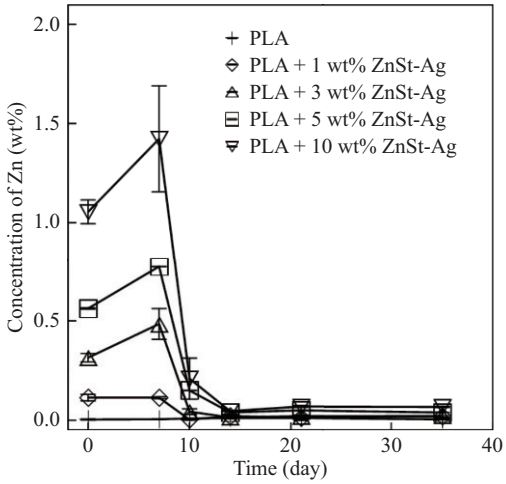

Fig. 7 Concentration of Zn in the composites during abiotic hydrolysis

concentration of Zn fell to nearly zero. The element Zn in this case included zinc stearate, as well as any other possible degradation product containing Zn which might have formed during hydrolysis. These results indicated that once degradation reached a certain degree, such compounds became highly mobile in the matrix and were able to diffuse out rapidly. Such quick diffusion of the zinc components supports the results derived from biodegradation, in which mineralization was enhanced by increasing the concentration of the additive.

CONCLUSIONS

Initially, the composites of PLA and hybrid particles of zinc stearate and silver were prepared by thermoplastic processing; the levels of ZnSt-Ag concentration equalled 1 wt%, 3 wt%, 5 wt% and 10 wt%. As expected, thermal degradation of the PLA occurred during processing, in parallel with a certain stabilization effect by ZnSt-Ag, which was detected through recording a lesser reduction in M_w. Analysing thermal properties revealed a slight decrease in T_g from 56 °C (for neat PLA) to approximately 50 °C, whereas for the samples with 3 wt%, 5 wt% and 10 wt% of ZnSt-Ag, the melting endotherm was recorded at around 117 °C, which was ascribed to contribution by the filler. The PLA matrix was amorphous, and no crystallization was observed during DSC runs.

Antimicrobial activity was evident, even at concentrations of ZnSt-Ag. Indeed, the bacterial colonies were reduced to approximately 30%. However, the most significant activity was exhibited by the system with 10 wt% of filler. Furthermore, the drastic improvement in mechanical properties, especially elongation at break, was achieved by adding 10 wt% ZnSt-Ag. The initial elongation of neat PLA equalled approximately 15%, but after incorporating the filler the value increased to almost 40% of elongation.

ZnSt-Ag did not play a significant role in the rate of abiotic hydrolysis of the PLA phase, at least not under the investigated conditions, with all samples exhibiting an M_w of around 6000 g·mol^{-1} after seven days of the experiment. Under biotic conditions, the presence of the additive promoted mineralization of the composite, although it was suggested that in this instance the more rapid mineralization observed immediately after composting could be attributed to mineralization of the additive rather than the PLA molecules. Measuring the contents of Ag and Zn in the composite during abiotic hydrolysis revealed minimal diffusion of Ag ions from the matrix, but highlighted the very extensive washing of Zn-related compounds.

Electronic Supplementary Information

Electronic supplementary information (ESI) is available free of charge in the online version of this article at http://dx.doi.org/10.1007/s10118-018-2120-0.

ACKNOWLEDGMENTS

This work was financially supported by the Czech Science Foundation (No. 17-16928Y) and by the Ministry of Education, Youth and Sports of the Czech Republic within the NPU I programme (No. LO1504).

REFERENCES

1 Izundia, E.; Larranaga, A.; Vilas, J. L.; Leon, L. M. Three-dimensional orientation of poly (L-lactide) crystals under uniaxial drawing. RSC Adv. 2016, 6(15), 11943−11951.
2 Imre, B.; Pukánszky, B. Compatibilization in bio-based and biodegradable polymer blends. Eur. Polym. J. 2013, 49(6), 1215−1233.
3 Jacobsen, S.; Fritz H. G. Plasticizing effect of different plasticizers on the mechanical properties of polylactide. Polym. Eng. Sci. 1999, 39(7), 1303−1310.
4 Mekonnen, T.; Mussone, P.; Khalil, H.; Bressler, D. Progress in bio-based plastics and plasticizing modifications. J. Mater. Chem. A 2013, 1(43), 13379−13398.
5 Martin, O.; Averous, L. Poly(lactic acid): plasticization and properties of biodegradable multiphase systems. Polymer 2001, 42(14), 6209−6219.
6 Maglio, G.; Malinconico, M.; Migliozzi, A.; Groeninckx, G. Immiscible poly(L-lactide)/poly(ε-caprolactone) blends: influence of the addition of a poly (L-lactide)-poly

(oxyethylene) block copolymer on thermal behavior and morphology. Macromol. Chem. Phys. 2004, 205(7), 946−950.
7 Maglio, G.; Migliozzi, A.; Palumbo, R. Thermal properties of di- and triblock copolymers of poly(L-lactide) with poly(oxyethylene) or poly(ε-caprolactone). Polymer 2003, 44(2), 369−375.
8 Maglio, G.; Migliozzi, A.; Palumbo, R.; Immirzi, B.; Grazia Volpe, M. Compatibilized poly(ε-caprolactone)/poly(L-lactide) blends for biomedical uses. Macromol. Rapid Commun. 1999, 20(4), 236−238.
9 Galya, T.; Sedlarik, V.; Kuritka, I.; Sedlarikova, J.; Saha, P. Characterization of antibacterial polymeric films based on poly (vinyl alcohol) and zinc nitrate for biomedical applications. International Journal of Polymer Analysis and Characterization[online]. 2008, 13(4), 241−253.
10 Iqbal, N.; Kadir, M. R. A.; Nik Malek, N. A. N.; Mahmood, N. H.; Murali, M. R.; Kamarul, T. Rapid microwave assisted synthesis and characterization of nanosized silver-doped hydroxyapatite with antibacterial properties. Mater. Lett. 2012, 89, 118−122.
11 Bazant, P.; Munster, L.; Machovsky, M.; Sedlak, J.; Pastorek, M.; Kozakova, Z.; Kuritka, I. Wood flour modified by hierarchical Ag/ZnO as potential filler for wood-plastic composites with enhanced surface antibacterial performance. Ind. Crops Prod. 2014, 62, 179−187.
12 Breitwieser, D.; Moghaddam, M. M.; Spirk, S.; Baghbanzadeh, M.; Pivec, T.; Fasl, H.; Ribitsch, V.; Kappe, C. O. *In situ* preparation of silver nanocomposites on cellulosic fibers-microwave *vs* conventional heating. Carbohydr. Polym. 2013, 94(1), 677−686.
13 Zhao, X.; Xia, Y.; Li, Q.; Ma, X.; Quan, F.; Geng, C.; Han, Z. Microwave-assisted synthesis of silver nanoparticles using sodium alginate and their antibacterial activity. Colloids Surf. A: Physicochem. Eng. As. 2014, 144, 180−188.
14 Pantani, R.; Gorrasi, G.; Vigliotta, G.; Murariu, M.; Dubois, P. PLA-ZnO nanocomposite films: Water vapor barrier properties and specific end-use characteristics. Eur. Polym. J. 2013, 49(11), 3471−3482.
15 Kucharczyk, P.; Pavelková, A.; Stloukal, P.; Sedlarík, V. Degradation behaviour of PLA-based polyesterurethanes under abiotic and biotic environments. Polym. Degrad. Stab. 2016, 129(1), 222−230.
16 Stloukal, P.; Kucharczyk, P. Acceleration of polylactide degradation under biotic and abiotic conditions through utilization of a new, experimental, highly compatible additive. Polym. Degrad. Stab. 2017, 142(1), 217−225.
17 Lipik, V. T; Widjaja, L. K.; Liow, S. S.; Venkatraman, S. S. Effects of transesterification and degradation on properties and structure of polycaprolactone-polylactide copolymers. Polym. Degrad. Stab. 2010, 95, 2596−2602.
18 Undri, A.; Rosi, L.; Frediani, M.; Frediani, P. Conversion of poly(lactic acid) to lactide *via* microwave assisted pyrolysis. J. Anal. Appl. Pyrolysis 2014, 110, 55−65.
19 Salazar, R.; Domenek, S.; Plessis, C.; Ducruet, V. Quantitative determination of volatile organic compounds formed during polylactide processing by MHS-SPME. Polym. Degrad. Stab. 2017, 136, 80−88.
20 Badia, J. D.; Santonja-Blasco, L.; Moriana, R.; Amparo, R. G. Thermal analysis applied to the characterization of degradation in soil of polylactide: II On the thermal stability and thermal decomposition kinetics. Polym. Degrad. Stab. 2010, 95(1), 2192−2199.
21 Wang, M.; Xu, J.; Wu, H.; Guo, S. Effect of pentaerythritol and organic tin with calcium/zinc stearates on the stabilization of poly(vinyl chloride). Polym. Degrad. Stab. 2006, 91(9), 2101−2109.
22 Rosa, D. S.; Grillo, D.; Bardi, M. A. G.; Calil, M. R.; Guedes, C. G. F.; Ramires, E. C.; Frollini, E. Mechanical, thermal and morphological characterization of polypropylene/biodegradable polyester blends with additives. Polym. Test. 2009, 28(8), 836−842.
23 Farah, S.; Anderson, D. G.; Langer, R. Physical and mechanical properties of PLA, and their functions in widespread applications-A comprehensive review. Adv. Drug Deliv. Rev. 2016, 107, 367−392.
24 Da Costa, H. M.; Abrantes T. A. S.; Nunes, R. C. R.; Visconte, L. L. Y.; Furtado, C. R. G. Design and analysis of experiments in silica filled natural rubber compounds-effect of castor oil. Polym. Test. 2003, 22(7), 769−777.
25 Cam, D.; Marucci, M. Influence of residual monomers and metals on poly(L-lactide) thermal stability. Polymer 1997, 38(8), 1879−1884.
26 White, R. P.; Lipson, J. E. G. Polymer free volume and its connection to the glass transition. Macromolecules 2016, 49(11), 3987−4007.
27 Eili, M.; Shameli, K.; Ibrahim, N. A.; Wan Yunus, W. M. Z. Degradability enhancement of poly(lactic acid) by stearate-Zn3Al LDH nanolayers. Int. J. Mol. Sci. 2012, 13(12), 7938−7951.
28 Jiang, L. J.; Zhang, J.; Wolcott, M. P. Comparison of polylactide/nano-sized calcium carbonate and polylactide/ montmorillonite composites: Reinforcing effects and toughening mechanisms. Polymer 2007, 48(26), 7632−7644.
29 Shankar, S.; Rhim, J. V. Tocopherol-mediated synthesis of silver nanoparticles and preparation of antimicrobial PBAT/silver nanoparticles composite films. LWT-Food Sci. Technol. 2016, 72, 149−156.
30 Egger, S.; Lehman, R. P.; Height, M. J.; Loessner, M. J.; Schuppler, M. Antimicrobial properties of a novel silver-silica nanocomposite material. Appl. Environ. Microbiol. 2009, 75(9), 2973−2976.
31 Shen, Y. CHEN, Z.; Hou, Z.; Li, T.; Lu, X. Ecotoxicological effect of zinc oxide nanoparticles on soil microorganisms. Front. Environ. Sci. Eng. 2015, 9(5), 912−918.
32 Dhas, S. P.; Shiny, P. J.; Khan, S.; Mukherjee, A.; Chandrasekaran, N. Toxic behavior of silver and zinc oxide nanoparticles on environmental microorganisms. J. Basis. Microbiol. 2014, 54(9), 916−927.

https://doi.org/10.1007/s10118-018-2120-0